

# Fast 3D Spiral Chemical Shift Imaging of Mitochondrial Metabolism in Brain with C6 Glioma using Hyperpolarized [2-<sup>13</sup>C]Pyruvate

Jae Mo Park<sup>1,2</sup>, Sonal Josan<sup>1,3</sup>, Taichang Jang<sup>4</sup>, Milton Merchant<sup>4</sup>, Ronald Watkins<sup>1</sup>, Yi-Fen Yen<sup>1</sup>, Ralph Hurd<sup>5</sup>, Lawrence Recht<sup>4</sup>, Daniel Spielman<sup>1,2</sup>, and Dirk Mayer<sup>1,3</sup>  
<sup>1</sup>Radiology, Stanford University, Stanford, California, United States, <sup>2</sup>Electrical Engineering, Stanford University, Stanford, California, United States, <sup>3</sup>Neuroscience Program, SRI International, Menlo Park, California, United States, <sup>4</sup>Neurology and Neurological Science, Stanford University, Stanford, California, United States, <sup>5</sup>Applied Science Laboratory, GE Healthcare, Menlo Park, California, United States

**Target Audience** Those who investigate mitochondrial metabolism using MR spectroscopic imaging (MRSI)

**Purpose** Metabolic imaging of hyperpolarized [1-<sup>13</sup>C]pyruvate (Pyr) has been successfully applied to cancer imaging as it is sensitive to the Warburg effect, i.e., the shift from oxidative phosphorylation (OXPHOS) towards glycolysis (GLY) [1]. The main focus has been on increased GLY as observed by increased labeling of [1-<sup>13</sup>C]lactate (Lac). Imaging of <sup>13</sup>C-bicarbonate, reflecting flux through Pyr dehydrogenase (PDH) from Pyr to acetyl coenzyme A (acetyl-CoA), was suggested as a surrogate marker for OXPHOS [2], but could not be used to assess tricarboxylic acid (TCA) cycle because the label is released as <sup>13</sup>CO<sub>2</sub> in the conversion from Pyr to acetyl-CoA, which has multiple alternative pathways besides the TCA cycle, e.g., fatty acid metabolism. Recently, [2-<sup>13</sup>C]Pyr, where the labeled carbon is retained in the conversion to acetyl-CoA, has been successfully exploited to observe mitochondrial metabolism of a healthy rat brain by detecting [5-<sup>13</sup>C]glutamate (Glu) and [1-<sup>13</sup>C]acetyl-carnitine (ALCAR) [3]. However, metabolic imaging of hyperpolarized [2-<sup>13</sup>C]Pyr is challenging due to the large dispersion of the chemical shift (CS), e.g., ~4500 Hz between [2-<sup>13</sup>C]Pyr and [2-<sup>13</sup>C]Lac at 3 T, leading to a large CS displacement artifact (CSDA) when using slice-selective pulses. In this study we developed a fast volumetric chemical shift imaging (CSI) sequence for imaging of hyperpolarized [2-<sup>13</sup>C]Pyr and its products, and applied it to measuring brain metabolism in healthy and C6 glioma-bearing rats.

**Methods** To overcome the problem of CSDA, a non-selective hard pulse was used for signal excitation followed by a 3D spiral CSI readout. To reduce the number of spatial interleaves, spectral undersampling [4] was applied while avoiding spectral overlap for the resonances of interest exploiting the spectral sparsity. All measurements were performed on a clinical 3-T GE MR scanner with a custom-built insert gradient coil (500 mT/m, 1856 mT/m/ms). A <sup>13</sup>C surface coil (Ø<sub>inner</sub> = 28 mm) was used for both RF excitation and signal reception, and a proton birdcage coil (Ø = 70mm) was used to acquire a reference proton MRI. Four healthy (287-337 g) and two C6 glioma-bearing (200-215 g) male Wistar rats were anesthetized with 1-3 % isoflurane in oxygen (~1.5 L/min). For the tumor-implanted rats, approximately 10<sup>6</sup> C6 rat glioma cells were injected into the right hemisphere of brains 10 days prior to the <sup>13</sup>C experiment. MRSI data were acquired using the 3D spiral CSI 25 s after the start of each Pyr injection (1.56 mmol/kg body weight of 125-mM solution) through a tail vein catheter. For the detection of [5-<sup>13</sup>C]Glu and [2-<sup>13</sup>C]Lac, a spectral width (SW) of 1042 Hz was chosen (Fig. 1). Other acquisition parameters were: pulse width = 56 µs, flip angle = 9.8° per excitation, FOV = 43.5 x 43.5 x 64.8 mm<sup>3</sup>, matrix size = 16 x 16 x 12, 5 spatial interleaves, 96 echoes, T<sub>acq</sub> = 5.6 s. A second set of parameters was used for imaging of [1-<sup>13</sup>C]ALCAR: SW = 890 Hz, 4 spatial interleaves, T<sub>acq</sub> = 5.2 s. Dichloroacetate (DCA) was administered (200 mg/kg body weight dissolved in 30

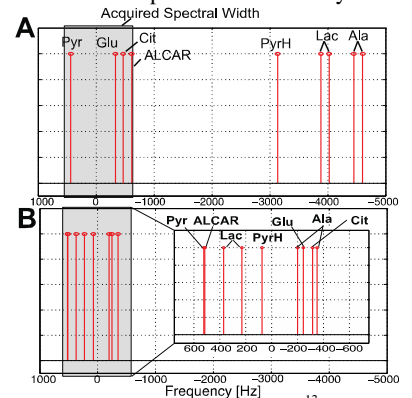


**Fig.1** Spectral distributions of [2-<sup>13</sup>C]Pyr and its products in (A) full SW and (B) narrowed (1042 Hz, shaded region) SW with aliasing used for [5-<sup>13</sup>C]Glu detection

g/mL of saline) to increase Pyr flux through PDH. Metabolite maps were calculated as previously described [3] and normalized to maximum Pyr signal.

**Results** Metabolite maps of Pyr, Lac, and Glu from a tumor-bearing rat at baseline and 1 h after DCA administration are shown in Fig. 2. The baseline maps (averaged over two Pyr injections) clearly show higher Lac in the tumor reflecting the increased GLY. The tumor also has lower Glu (in fast exchange with the TCA cycle intermediate α-ketoglutarate) indicating reduced amount of acetyl-CoA entering the TCA cycle compared to normal brain. Administration of DCA lead to an increase in Glu due to increased conversion of Pyr to acetyl-CoA (Glu/Pyr ratio increased 0.018 ± 0.002 to 0.031 ± 0.004 in healthy rat brain, n = 3, P = 0.02). The metabolite map of ALCAR in Fig. 3 (generated from acetyl-CoA) from a healthy rat post-DCA indicates that ALCAR is primarily observed in the muscle/fat tissue surrounding the brain. Pre-DCA ALCAR level was too low to generate images.

**Discussion** The proposed pulse sequence permits metabolic imaging of hyperpolarized [2-<sup>13</sup>C]Pyr and its metabolic products without CSDA. Because spectral undersampling is applied, not all metabolic products can be detected within the same acquisition. Although Pyr overlaps with ALCAR using a SW of 1042 Hz, the effect on Pyr quantification can be neglected as Pyr is much larger than ALCAR and the latter is predominantly found outside the brain. As a non-selective hard pulse is used for excitation, the FOV has to be at least as large as the sensitive volume of the receive coil.

**Conclusion** By permitting the simultaneous detection of Pyr, Lac, and Glu, the proposed sequence allows for the observation of metabolic pathways altered in cancer metabolism. The method should be useful in assessing the response to cancer treatment, in particular for therapies that target the altered balance between GLY and OXPHOS.

**References** [1] Kurhanewicz J, et al. *Neoplasia* 2011;13:81-97, [2] Park JM, et al. *ISMRM* 2012;4312, [3] Park JM, et al. *ISMRM* 2012;4323, [4] Mayer D, et al. *MRM* 2009;62:557-564

**Acknowledgements** NIH: EB009070, AA005965, AA0018681, AA13521-INIA, P41 EB015891, DOD: PC100427, Lucas Foundation, Nadia's gift, and GE Healthcare

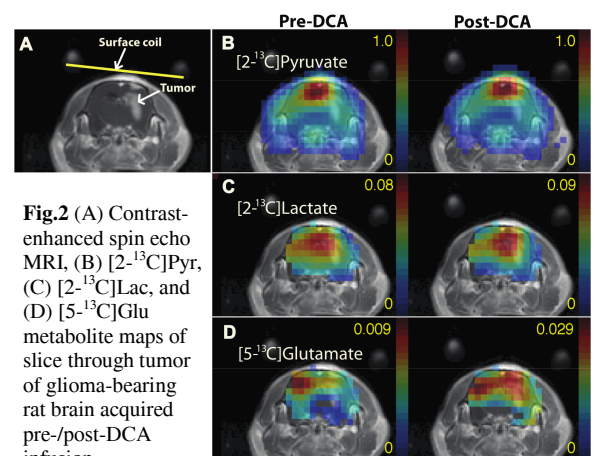


**Fig.2** (A) Contrast-enhanced spin echo MRI, (B) [2-<sup>13</sup>C]Pyr, (C) [2-<sup>13</sup>C]Lac, and (D) [5-<sup>13</sup>C]Glu metabolite maps of slice through tumor of glioma-bearing rat brain acquired pre-/post-DCA infusion

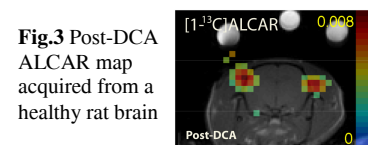


**Fig.3** Post-DCA ALCAR map acquired from a healthy rat brain